Simulating land surface processes in Cabauw super-site with ECLand surface model: diurnal cycle to interannual variability

Luís Fróis[1], P.M.A. Miranda[1], Emanuel Dutra[1,2], Mariska Koning[3]

[1]Instituto Dom Luiz (IDL), University of Lisbon, Campo Grande, 1749-016, Lisbon, Portugal.
[2]Instituto Português do Mar e da Atmosfera (IPMA), Rua C do Aeroporto, 1749-077, Lisbon, Portugal.
[3]Royal Netherlands Meteorological Institute KNMI, PO Box 201, 3730 AE, De Bilt, Netherlands.

INSTITUTO DOM LUIZ
Koninklijk Nederlands Meteorologisch Instituut
Ministerie van Infrastructuur en Waterstaat
IPMA
fct Fundação para a Ciência e a Tecnologia
Sharing is encouraged
EGU General Assembly
Session CL4.1 – Land-atmosphere interactions and climate extremes

Introduction

Land surface models (LSMs) are an essential component of weather and climate models. They simulate surface-atmosphere exchanges of water, energy, and carbon. Energy fluxes are represented by partitioning available energy (net radiation minus ground heat flux, Rnet-Qg) into turbulent fluxes of latent and sensible heat (Qle, Qh).

Qle, representing evaporation (E), is the most challenging surface energy budget (SEB) term to simulate. One reason is that plant transpiration is limited by stress-induced stomatal closure, represented by canopy resistance (r_c), which depends on environmental conditions.

Objectives

- Evaluate the SEB representation in ECMWF's LSM, ECLand, against in-situ observations from Cabauw meteorological observatory (Netherlands).
- Use ECLand to study the importance of plant stress due to soil moisture (SM) and vapour pressure deficit (VPD) for energy partitioning.

Model description

ECLand computes evaporation from the surface-atmosphere humidity gradient $\Delta q = q_{sat}(T_{skin}) - q$, with an aerodynamic resistance r_a. For plant transpiration, r_c is added as an extra resistance:

$$E = \frac{\rho_{air}}{r_a + r_c}\Delta q$$

r_c incorporates the effects of solar radiation (R_s), SM (θ), and VPD (D_a) through a multiplicative scheme:

$$r_c = \frac{r_{S,min}}{LAI} f_R(R_s) f_\theta(\theta) f_D(D_a)$$

The SM stress factor is defined between the wilting point (pwp) and field capacity (fc):

$$\frac{1}{f_\theta(\theta)} = \begin{cases} 0, & \theta < \theta_{pwp} \\ \left(\dfrac{\theta - \theta_{pwp}}{\theta_{fc} - \theta_{pwp}}\right)^{g_\theta}, & \theta_{pwp} \le \theta \le \theta_{fc} \\ 1, & \theta > \theta_{fc} \end{cases}$$

The VPD factor varies exponentially with D_a:

$$\frac{1}{f_D(D_a)} = \exp(-g_D D_a)$$

where $D_a = e_{sat} - e$, the difference between saturation and actual vapour pressure.

Methods

Point simulations with ECLand for Cabauw, 2001-2020 (20 years).
Land cover is set to 100% grassland, reflecting site characteristics.
Five configurations are tested, in addition to the default, **Ctr** (**Table 1**):

- Experiments **1**, **2**, **3**, **4**: reduced r_c, with different dependence on SM/VPD.
- Experiment **5**: increased soil vertical resolution, with 9 layers instead of 4.

Variables evaluated:

- SEB terms:
  - Rnet, Qg, Qh, Qle.
  - Surface thermal radiation (LWup).
  - Evaporative fraction: EF = Qle/(Qh+Qle).
- Soil temperature (TS) profile.

Types of evaluation:

- Summer diurnal cycles
- Annual cycles
- Summer interannual variability

Table 1 – Configurations of ECLand Simulations

Simulation name	SM exponent g_θ	VPD coefficient g_D [hPa^{-1}]	Number of soil layers n_z
Ctr_sm1_vpd0 (default configuration)	1 (linear function of θ)	0 (no VPD stress)	4
Exp1_sm0_vpd0	0 (no SM stress)	0	
Exp2_sm0_vpd003		0.03	
Exp3_sm025_vpd0	0.25	0	
Exp4_sm025_vpd003		0.03	
Exp5_nz9	1	0	9

Results and Discussion

The default model configuration (**Ctr**) underestimates (overestimates) summer daytime Qle (Qh) (**Fig. 1**). The diurnal cycle of Qg shows a large overestimation by night and day. LWup has a daytime cold bias.

Exp1 (no stress from either SM or VPD) overcorrects the Qle/Qh errors, overestimating Qle. **Exp2**, **Exp3** and **Exp4** (intermediate r_c) have better agreement of Qle/Qh cycle mean and amplitude (**Fig. 2**). However, they increase LWup bias, by increasing evaporative cooling.

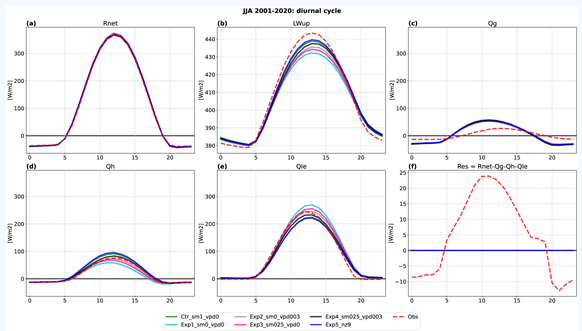

Fig. 1 – Mean diurnal cycles, for JJA 2001-2020, of **(a)-(e)** observed and simulated SEB terms; **(f)** SEB residual. Hours on x-axis are UTC.

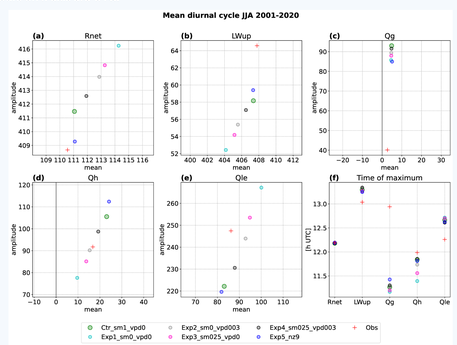

Fig. 2 – Parameters of the diurnal cycles in **Fig. 1**: **(a)-(e)** Mean and amplitude [W m^{-2}]; **(f)** estimated peak time.

The annual cycles (**Fig. 3**) show the same patterns as the diurnal cycles from mid-spring to mid-autumn. The Qh/Qle partition is represented by EF, which is underestimated by **Ctr** and well reproduced by **Exp2** and **Exp3**.
In winter, the errors are smaller because the fluxes are small, and the experiments have no effect because evaporation is not limited by plant stress. EF rises in winter, due to small Qh.

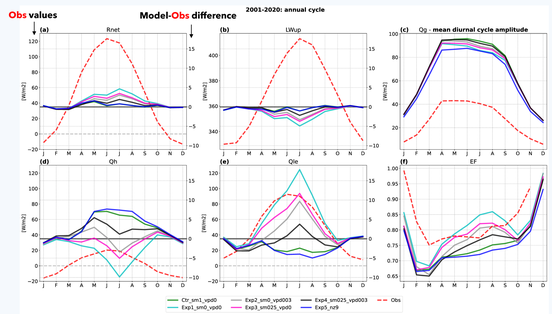

Fig. 3 – Mean annual cycles, averaged over JJA 2001-2020, of observed and simulated SEB terms. Second y-axis indicates differences from **Obs**. In **(c)** and **(f)**, only absolute values are shown.

The simulated soil temperature diurnal cycles show an overestimated amplitude and a phase lead, at all depths (**Fig. 4**). This is consistent with the Qg amplitude overestimation, as in ECLand Qg is driven by thermal contrast between the soil and the skin layer.
Increasing vertical resolution (**Exp5**) reduces TS amplitude and phase errors. On SEB partitioning, Exp5 has negligible effects, except for a slight improvement of Qg (**Fig. 3**).

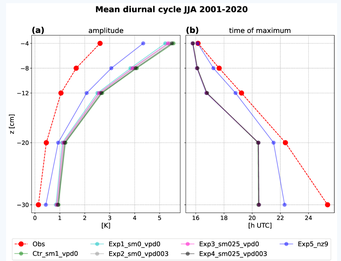

Fig. 4 – Amplitude and phase of soil temperature summer diurnal cycle, for 5 levels (shown in y-axis as depth relative to the surface).

The summer interannual variability of Qh and EF is well represented in **Ctr**, although Qle is not (**Table 2**). Experiments 1-4 show statistically significant Qle correlations, but Qh is poorly correlated with Obs in **Exp3**, and uncorrelated in **Exp1** and **Exp2**. **Exp4** has the best overall performance.

Finally, we study an error source in Cabauw soil observations. Soil sensors are known to sink over the years (Bosveld, 2020), which may cause them to register lower diurnal amplitudes (see **Fig. 4a**).
They were reinstalled in July 2016. Before this, the observed diurnal cycle amplitude of Qg and TS shows a negative trend, and afterwards a large jump (**Fig. 5**). The simulations do not show these patterns.
Fig. 5 suggests that the model's Qg and TS overestimation is real but exaggerated by this error.

Table 2 – Interannual correlation of JJA means between **Obs** and each simulation. For Qg and LWup, we used the mean diurnal cycle amplitudes for each summer. Statistically significant correlations at a 99% level are underlined.

	Qh	Qle	EF	LWup	Qg
Ctr_sm1_vpd0	**0.80**	0.21	**0.68**	**0.88**	0.22
Exp1_sm0_vpd0	-0.28	**0.65**	-0.45	**0.87**	0.13
Exp2_sm0_vpd003	0.00	**0.67**	-0.33	**0.88**	0.14
Exp3_sm025_vpd0	0.41	**0.70**	0.05	**0.89**	0.16
Exp4_sm025_vpd003	**0.72**	**0.72**	0.52	**0.90**	0.17

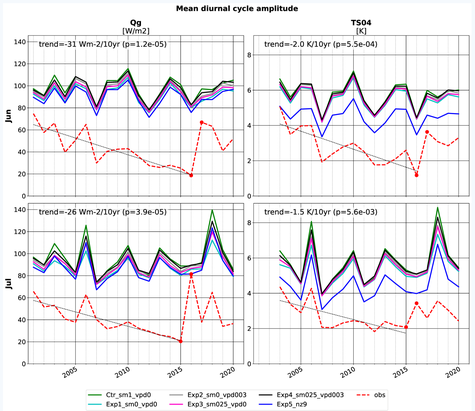

Fig. 5 – Interannual evolution of mean diurnal cycle amplitude of Qg and 4 cm depth temperature, for June and July.

Summary/Conclusions

ECLand underestimates daytime Qle and overestimates Qh for Cabauw in summer, corresponding to a low EF. The Qg diurnal cycle is overestimated, but the error is partly due to a gradual decrease in observed amplitude.

Eliminating SM and VPD stress produces unrealistic results, while moderate r_c reductions improve Qh/Qle partitioning. Interannual variability is strongly impacted, but all simulations show shortcomings.

No simulation is optimal; indeed, in this study we do not intend to propose changes to the model. However, the results show the importance of SM and VPD stress formulations to simulate surface energy partitioning.

Future work

We will complete this work by considering the large observational uncertainty due to SEB imbalance: the residual Res = Rnet-Qg-Qh-Qle.
In the present version, we use a corrected version of Qle that "absorbs" part of Res (proportionally to EF). Using raw eddy-covariance Qle, summer Res in **Fig. 1f** would reach 80 W m^{-2}.
Our plan is to use EF-corrected Qh and Qle for the evaluation, with error bars of length Res, and the raw observations as one extreme.

Bosveld, F. C. (2020). *The Cabauw in-situ observational program 2000-present: Instruments, calibrations and set-up*. (Technical Report TR-384). De Bilt: KNMI.

Acknowledgements | This work was developed as part of Luís Fróis's PhD, with funding from the Portuguese Fundação para a Ciência e a Tecnologia (FCT) through the Grant No. 2020.08478.BD. The authors also acknowledge the financial support of FCT I.P./MCTES through national funds (PIDDAC) – UIDB/50019/2020 – IDL. Our thanks to Anton Beljaars (ECMWF) for his comments and suggestions, and to Fred Bosveld (KNMI) for his guidance in our use of Cabauw observations.

Email: lhfrois@fc.ul.pt